Characterisation of shallow groundwater dissolved organic matter in aeolian, alluvial and fractured rock aquifers

Liza K. McDonough [a,b,*], Helen Rutlidge [a,c], Denis M. O'Carroll [a,c],
Martin S. Andersen [a,c], Karina Meredith [d], Megan I. Behnke [e,f],
Robert G.M. Spencer [e,f], Amy M. McKenna [f], Christopher E. Marjo [g],
Phetdala Oudone [a,b], Andy Baker [a,b]

[a] Connected Waters Initiative Research Centre, UNSW Sydney, NSW 2052, Australia
[b] School of Biological, Earth and Environmental Sciences, UNSW Sydney, NSW 2052, Australia
[c] School of Civil and Environmental Engineering, UNSW Sydney, NSW 2052, Australia
[d] Australian Nuclear Science and Technology Organisation (ANSTO), New Illawarra Rd, Lucas Heights, NSW 2234, Australia
[e] Department of Earth, Ocean, and Atmospheric Science, Florida State University, FL 32310, USA
[f] National High Magnetic Field Laboratory, Florida State University, Tallahassee, FL 32310-4005
[g] Mark Wainwright Analytical Centre, UNSW, Sydney, NSW 2052, Australia

Abstract

Groundwater organic matter is processed within aquifers through transformations such as the adsorption of dissolved organic matter (DOM) to minerals and biodegradation. The molecular character of DOM varies according to its source and this can impact its bioavailability and reactivity. Whilst the character of DOM in riverine and oceanic environments is increasingly well understood, the sources, character and ultimately the fate of groundwater DOM remains unclear. Here we examine groundwater DOM from contrasting hydrogeological settings in New South Wales, Australia. For the first time, we identify the distinct molecular composition of three groundwater DOM end-members including a modern terrestrial input, an aged sedimentary peat source, and an aged stable by-product pool. We also identify and characterise the processing pathway of DOM in semi-arid, low sedimentary organic carbon (OC) environments. Based on size exclusion chromatography, ultrahigh-resolution Fourier-transform ion cyclotron resonance mass spectrometry (FT-ICR MS), isotopic analyses (^{13}C, ^{14}C and ^{3}H) and principle component analysis (PCA), we show that in higher rainfall temperate coastal peatland environments, large amounts of aged sedimentary organic carbon can leach into groundwater resulting in higher molecular weight (500 g mol^{-1} < molecular weight > 1000 g mol^{-1}) and highly aromatic groundwater DOM with high O/C ratios and low H/C ratios. We show that in semi-arid environments with low rainfall rates and high groundwater residence times, groundwater dissolved organic carbon (DOC) is processed into increasingly low molecular weight (<350 g mol^{-1}), low aromaticity DOM with low O/C ratios and high H/C ratios by subsurface processing mechanisms such as biodegradation and adsorption. We provide the first comprehensive study of groundwater DOM characterisation based on multiple analytical techniques, and highlight the impact of source inputs and processing on groundwater DOM composition at a molecular level.
Crown Copyright © 2020 Published by Elsevier Ltd. All rights reserved.

* Corresponding author at: School of Biological, Earth and Environmental Sciences, UNSW Sydney, NSW 2052, Australia.
E-mail address: lizamcdonough@gmail.com (L.K. McDonough).

1. INTRODUCTION

Dissolved organic matter (DOM) plays a significant role in carbon cycling and biogeochemical and ecological functioning (Schiff et al., 1990; Banwart 1999; Burrows et al., 2017; King et al., 2018; Johannesson et al., 2019; Li et al., 2019; Wegner et al., 2019) and is an important component of groundwater quality. Understanding groundwater DOM sources and processing mechanisms can allow for better quantification of the role of groundwater DOM in the terrestrial carbon budget (Battin et al., 2009). Groundwater DOM composition also has implications for water quality parameters that are driven by DOM degradation (e.g. dissolved oxygen, ferrous iron and arsenic (Appelo and Postma, 2005)) which may have implications for human health (Evans et al., 2019). Furthermore, subsurface DOM processing has been shown to drive stream ecosystem food-webs (Burrows et al., 2018). Research is needed to quantify these processes and their rates in groundwater, and how they may vary over time and space due to hydrologic and external water quality changes. Recent studies have investigated DOM molecular composition correlated to reactivity in surface waters, including oceans (Reemtsma et al., 2008; Lechtenfeld et al., 2014), riverine (Stubbins et al., 2010; Kaiser et al., 2017), glacial (Grannas et al., 2006; Spencer et al., 2014), and lake water (Kellerman et al., 2014; Kellerman et al., 2015). Few investigations correlate groundwater DOM composition to source identification or processing pathways (Longnecker and Kujawinski, 2011; Lechleitner et al., 2017).

The molecular character of DOM (Lechtenfeld et al., 2014; Kellerman et al., 2018), as well as environmental setting (Kellerman et al., 2014), affect DOM sources, reactivity and processing pathways. DOM in permafrost for example is characterised by a relatively large percent relative abundance (% RA) of aliphatic and peptide-like compound classes (Spencer et al., 2015; Feng et al., 2018; Wang et al., 2018) which has been shown to be highly biolabile (Spencer et al., 2015; Wang et al., 2018; Textor et al., 2019). These energy-rich groups are characterised by organic matter with high H/C ratios (>1.5). Aliphatics and peptides are largely photo-resistant and have even been shown to be photoproduced in rivers when DOM is exposed to irradiation (Stubbins et al., 2010). Due to their rapid processing however, they are usually a relatively minor component (<10%) of DOM in aquatic environments (Kellerman et al., 2018) and it is likely that these compounds would not be present in high concentrations in processed groundwaters due to their biolability and the lack of UV exposure required to produce these compounds by photodegradation. In contrast, aromatic DOM groups have been identified in stream water exported from peatlands (Coward et al., 2018), and this has been shown to be less biolabile, but rapidly photodegraded or adsorbed to mineral surfaces (Jardine et al., 1989; Kaiser et al., 1996; Stubbins et al., 2010). These aromatic and polyphenolic groups are often leached from organic horizons high in vascular plant matter and can be a major component of soil pore water (O'Donnell et al., 2016). Flow path depths and position along an aquatic continuum also impact on DOM character (Raymond and Bauer, 2001; Sickman et al., 2010; Catalán et al., 2016; Barnes et al., 2018; Kellerman et al., 2018) with younger DOM typically less processed and associated with higher dissolved organic carbon (DOC) concentration, higher aromaticity, and shallow flow paths. Older DOM is typically more processed and has been associated with lower DOC, lower aromaticity, and deeper flow paths (Kaiser and Kalbitz, 2012). When elemental compositions are plotted as atomic ratios of H/C and oxygen to carbon O/C on a van Krevelen diagram, a highly stable subgroup of carboxyl-rich alicyclic molecules (CRAM) molecules in aquatic environments have been identified as being the potential stable end-products of DOM after extensive degradation (Hertkorn et al., 2006; Lechtenfeld et al. 2014; Kellerman et al., 2018). These CRAM molecules are predominantly located in a region of highly unsaturated and phenolic compounds (Kellerman et al., 2014).

Studies characterising DOM at a molecular level in groundwater are limited, which has restricted our ability to identify groundwater DOM sources and processing pathways. These degradation pathways are expected to differ from surface waters due to potentially greater exposure to mineral surfaces for adsorption, and a lack of photodegradation. Research has shown that DOM leached from organic horizons and soils typically has lower H/C and O/C ratios in groundwater compared to soil waters or surface waters due to biological and physical reactions in the vadose zone (Wassenaar et al., 1990). Furthermore, groundwater has been shown to contain a high relative proportion of carbon (C), hydrogen (H), oxygen (O) (CHO) containing molecular formulae, with research indicating that high levels of C, H, O and nitrogen (CHON) molecular formulae are possible in less biologically processed groundwater DOM (Longnecker and Kujawinski, 2011).

Here, we aim to determine the sources and controls on the molecular composition of groundwater DOM in two semi-arid inland alluvial and fractured rock aquifer environments and one coastal sand aquifer environment using ultrahigh-resolution Fourier-transform ion cyclotron resonance mass spectrometry (FT-ICR MS), size exclusion chromatography and isotopic analyses. We hypothesise that groundwater DOM sourced from surface waters will be of relatively low molecular weight due to pre-processing at the surface by photodegradation, adsorption and biodegradation. We expect that adsorption and biodegradation are major processing pathways of groundwater DOM, and hypothesise that further processing of DOM in groundwater will result in a decline in biolabile (aliphatic and peptide-like compounds) and easily adsorbed (aromatic, higher molecular weight) compounds. We also anticipate a relative increase in stable highly unsaturated and phenolic DOM compounds in groundwater as DOM is processed. In contrast, we hypothesise that groundwater DOM sourced from buried sedimentary organic matter in higher rainfall environments may contain aged, non-biolabile and unprocessed aromatic and polyphenolic DOM compounds of high molecular weight and high aromaticity. We anticipate that in environments where

sedimentary organic matter (OM) inputs are high, this source signal could dominate the character of aged groundwater DOM and overwhelm the processed DOM signal.

2. SAMPLING SITES

The study sites include one sedimentary organic carbon (OC)-rich coastal aeolian and marine sand aquifer site (Anna Bay, NSW) and two sedimentary OC-poor inland alluvial and fractured rock aquifer sites (Maules Creek and Wellington, NSW, Fig. 1). Both Wellington and Maules Creek are semi-arid sites, located just under 300 km inland from the coast and located 250 km apart. Groundwater samples obtained from these two inland sedimentary OC-poor environments were collected from dedicated research bores installed as part of the Australian
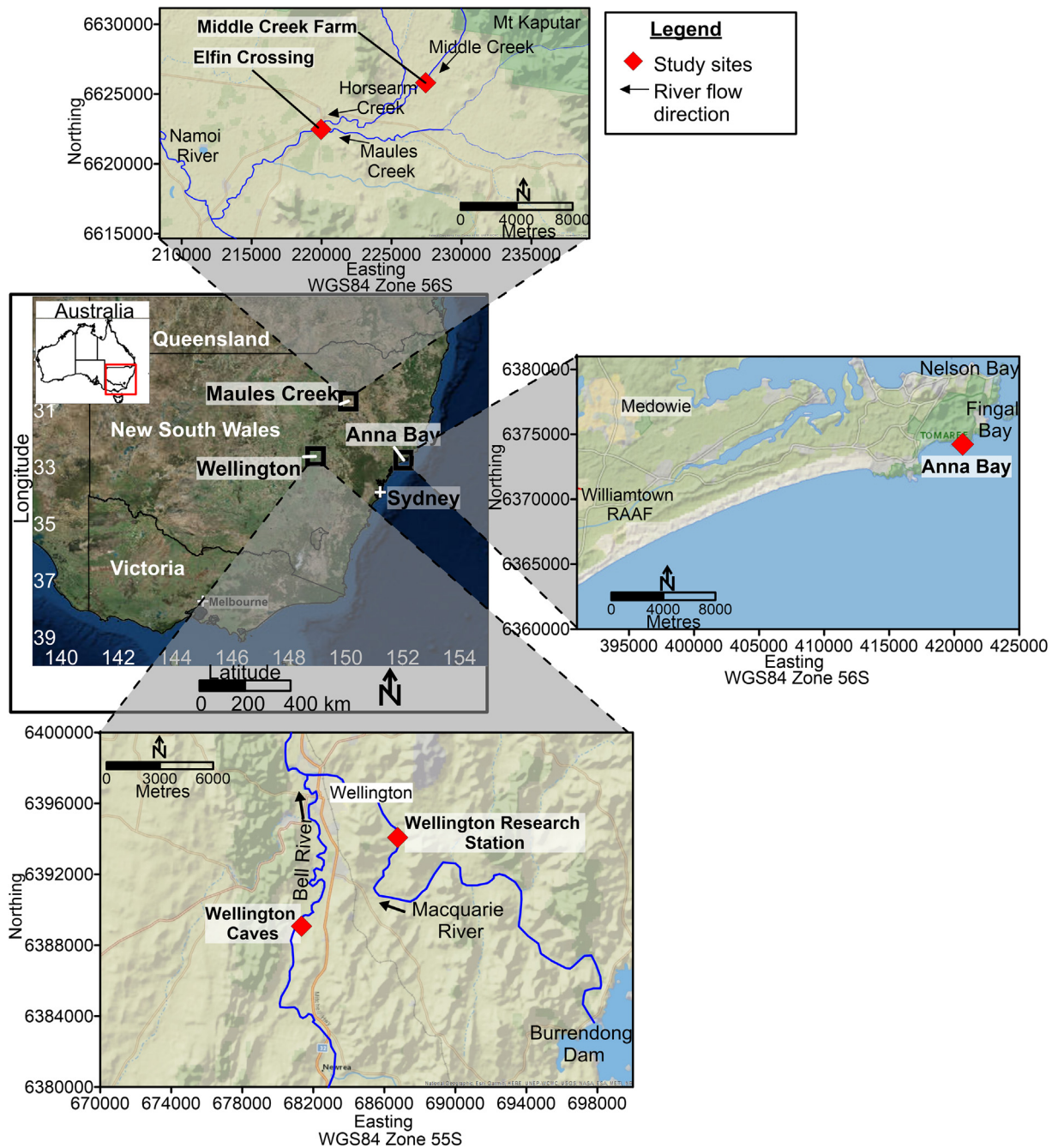

Fig. 1. Study areas at Wellington, Maules Creek and Anna Bay in New South Wales, Australia with sampling sites shown as red diamonds in insets. X-axis shows latitude (south), y-axis shows longitude (east) in geographic coordinates (decimal degrees) with insets shown in Universal Transverse Mercator coordinates in Zone 55S (Maules Creek) and Zone 56S (Wellington and Anna Bay). Relevant surface water flow directions are indicated by the black arrows.

National Collaborative Research Infrastructure Strategy (NCRIS) groundwater program, managed by the Connected Waters Initiative at the University of New South Wales, Sydney, Australia (UNSW). Each piezometer has a screened interval of 1 m or less allowing for depth-specific samples.

The sampling sites at Wellington and Maules Creek are located near streams (Fig. 1). Eight samples from Maules Creek were obtained from monitoring bores from different depths in the alluvial aquifer at Middle Creek farm, and from the alluvial aquifer and surface water at Elfin Crossing (see Table 1, Fig. S.1–Fig. S.3 and Appendix for more information). At Wellington, seven samples were collected in total from two rivers, the Bell River and Macquarie River, and from within the fractured rock and alluvial aquifers which dominate the area at two main Wellington sampling sites: Wellington Caves and Wellington Research Station (see Fig. 1, Fig. S.4–Fig. S.6 and Appendix for more information).

The sedimentary OC-rich temperate coastal site is located at Anna Bay, approximately 150 km north of Sydney, New South Wales (NSW), Australia (Fig. 1). Eight samples were obtained from a shallow aquifer near a wetland behind a dune system, approximately 500 m from the ocean, and from wells located in the sand dunes along a transect from the wetland to the shoreline (see Fig. S.7 and Appendix for further information). Water level data shows groundwater levels at Samurai Beach are largely controlled by precipitation (McDonough et al., 2020; Fig. S.8). There is a long-term trend of water movement from the wetland towards the dunes, to the coast (Fig. S.8) suggesting some bores may also be recharged by wetland surface water. Previous research has identified a peat layer at site S1 and S2 between 1 and 5 m bgs, and a clay unit at site S5 (Meredith et al., 2019). A summary of the study sites are shown in Table 1.

3. MATERIALS AND METHODS

3.1. Sampling

Major field campaigns were conducted for Wellington, Maules Creek and Anna Bay (on 15–16 August 2017, 11 October 2017, and 13–14 February 2018 respectively). Samples were collected to analyse for DOC, cations, anions, stable water isotopes, $\delta^{13}C$ and ^{14}C of DOC ($\delta^{13}C_{DOC}$ and $^{14}C_{DOC}$), $\delta^{13}C$ and ^{14}C of dissolved inorganic carbon ($\delta^{13}C_{DIC}$ and $^{14}C_{DIC}$), and ^{3}H. Sample sites were selected based on the availability and accessibility of monitoring bores suitable for groundwater sampling, their placement in transects from surface waters, and their relatively well-known recharge mechanisms. We utilised bore fields which were specifically designed to assist in understanding groundwater and surface water interactions. A mix of surface waters, shallow groundwaters, and deeper groundwater samples were selected based on available bore screen depths. Sample numbers were determined based on the availability and cost of ^{14}C and ^{3}H analyses. Discussion regarding the potential for seasonal variability to impact results or interpretation is provided in the Appendix.

Table 1
Summary of the geology, climate and number of samples obtained from each of the three research sites. Climate data is from Bureau of Meteorology. Information on weather station numbers and locations used is provided in the Appendix.

Geology	Climate	Samples taken
Maules Creek		
Quaternary alluvial sediment (gravels and clays) overlying Permian volcanics and coal measures[a,b,c]	Semi-arid climate with hot summers and mild winters. Annual average rainfall of 646 mm. Daily evaporation rates in summer and winter are 6.4 mm and 2.3 mm respectively.	Middle Creek: 2 × groundwater Elfin Crossing: 5 × groundwater, 1 × surface water
Wellington		
Quaternary alluvial deposits and colluvium, Devonian Garra Formation limestones, siltstones, shales, dolomitic limestones, clastic sequences, and Cuga Burga volcanics[d]	Temperate semi-arid climate. Relatively low, episodic rainfall uniformly distributed for most of the year. Hot summers and cold winters. Annual average rainfall of 616 mm. Daily evaporation rates in summer and winter are 7.5 mm and 1.7 mm respectively.	Wellington Caves: 2 × groundwater, 1 × surface water Wellington Research Station: 3 × groundwater, 1 × surface water
Anna Bay		
Unconsolidated aeolian and beach calcareous sand deposits containing peat layers[e]	Warm, temperate, humid climate. High rainfall year-round, with hot summers and mild winters. Annual average rainfall rate of 1346 mm. Daily evaporation rates in summer and winter are 11.8 mm and 2.9 mm respectively.	8 × groundwater samples

NB: Summer refers to the months December – February whilst winter refers to the months June – August.
[a] Andersen and Acworth (2009).
[b] Giambastiani et al. (2012).
[c] McCallum et al. (2013).
[d] Johnson (1975).
[e] Meredith et al. (2019).

Surface water samples (Macquarie River, Bell River and Maules Creek at Elfin Crossing) and shallow groundwater samples MLSA_40cm, MLSB_100cm and MLSD_115cm were obtained using a Series II Geopump peristaltic pump and a 10 mm diameter steel sampling spear with a 50 mm screen. A Monsoon 12 Volt Plastic Groundwater pump was used for deeper groundwater samples. Standing bore water levels were recorded using a dip meter, and in-field measurements of pH, temperature, electrical conductivity (EC) and dissolved oxygen (DO) were collected using an in-line Sheffield flow-cell attached to two Hach HQ40D multimeters for all samples. Groundwater samples were collected with the pump intake located just above the well screen after bores had been purged until in-field parameters had stabilised. Samples were collected for alkalinity, inorganic anions, cations, stable water isotopes, ^{3}H, ^{14}C$_{DIC}$, ^{14}C$_{DOC}$, δ^{13}C$_{DIC}$, δ^{13}C$_{DOC}$, DOC concentration, LC-OCD and FT-ICR MS.

All samples were filtered in the field to 0.45 μm, except for δ^{13}C$_{DIC}$ and δ^{13}C$_{DOC}$ samples which were filtered to 0.22 μm. Alkalinity samples were collected in 50 ml syringes prior to titration. Total alkalinity was determined by performing gran-titrations on 25 ml of each sample using sulfuric acid (H_2SO_4) at the end of each sampling day. Further information regarding sample quantities, storage and transport can be found in the Appendix.

3.2. Analysis

3.2.1. Isotopes

Samples were analysed for ^{14}C$_{DIC}$, ^{14}C$_{DOC}$, δ^{13}C$_{DIC}$, and ^{3}H at Australian Nuclear Science and Technology Organisation (ANSTO) in Sydney, NSW, Australia. Information on the methods used for the pre-treatment of samples for ^{14}C$_{DIC}$ and ^{14}C$_{DOC}$, as well as sample CO_2 extraction and graphitisation are summarised in the Appendix and described in Hua et al. (2001) and Bryan et al. (2017). Radiocarbon data are reported as percent Modern Carbon (pMC) normalised against the δ^{13}C, with an average 1σ error of the AMS readings that did not exceed ±0.56 pMC and ±0.42 pMC for ^{14}C$_{DOC}$ and ^{14}C$_{DIC}$ respectively. ^{14}C$_{DOC}$ (pMC) values were calculated using the ratio of ^{14}C/^{12}C with conventional radiocarbon ages rounded according to Stuiver and Polach (1977). Conversions from pMC to un-normalised ^{14}C$_{DIC}$ (pmc) values and Δ^{14}C$_{DOC}$ (‰) values were calculated as per Plummer and Glynn (2013).

Samples were analysed for ^{3}H at ANSTO. The sample is distilled to remove salts and organics prior to electrolytic concentration of ^{3}H. The samples, standards and blanks then have a current of <100 mA.cm^{-2} passed through it which allows for the removal of deuterium. Concentration is achieved through electrolysis over a period of 2 weeks. The concentrate is then distilled, and the sample analysed by liquid scintillation spectrometry using Perkin Elmer Quantulus™ instruments. Results were reported as tritium units (TU) with an uncertainty of ≤0.13 TU and a lower limit of detection of 0.06 TU.

Samples were analysed for δ^{13}C$_{DIC}$ by continuous-flow Delta V Advantage isotope ratio mass spectrometry (IRMS) at ANSTO using the methods described in Assayag et al. (2006). Results for δ^{13}C$_{DIC}$ are accurate to ±0.3 per mil (‰). Samples were analysed for δ^{13}C$_{DOC}$ at the UC Davis Stable Isotope Facility using an O.I. Analytical Model 1030 Total Organic Carbon Analyzer (Xylem Analytics, College Station, TX) interfaced to a PDZ Europa 20-20 isotope ratio mass spectrometer (Sercon Ltd., Cheshire, UK) utilizing a GD-100 Gas Trap Interface (Graden Instruments). Results for δ^{13}C$_{DOC}$ are accurate to ±0.5 ‰ for samples with DOC concentrations <1.2 mg C L^{-1}, and ±0.4 ‰ for samples with DOC concentrations >1.2 mg C L^{-1}. Results for both δ^{13}C$_{DIC}$ and δ^{13}C$_{DOC}$ were reported as per mil deviations from the international Vienna Pee Dee Belemnite (VPDB) standard.

Off-Axis Integrated Cavity Output Spectroscopy (OA-ICOS) was used to analyse stable water isotopes (^{2}H and ^{18}O) at UNSW using an LGR Liquid Water Isotope Analyser (Lis et al., 2008). A primary standard was run (VSMOW-2), with 5 further standards used to calibrate samples against. The maximum deviations were no larger than ±1.0‰ and ±0.2‰ for ^{2}H and ^{18}O respectively from the known reference material values.

3.2.2. Geochemistry

Anions and cations were analysed at the University of New South Wales (UNSW), Sydney using a Perkin Elmer Optima 7300 inductively coupled plasma (ICP) optical emission spectrometer and a Perkin Elmer NexION 300D ICP mass spectrometer. A Dionex IC system with an Ion-Pac AS14A analytical column was used to analyse fluoride, chloride, bromide, nitrite, nitrate, phosphate and sulphate. Single element High-Purity Standards™ were used to prepare multi-element standards at UNSW's Mark Wainwright Analytical Centre at concentrations of 0.2, 1, 10, and 100 mg L^{-1} and μg L^{-1}. A Lachat flow injection analyser (FIA) was used to analyse for nitrate and ammonium nitrogen (NO$_3$-N and NH$_4$-N). Mixed NO$_3^-$ and NH$_4^+$ standards at concentrations of 0.02, 0.05, 0.20, 0.50, 1.00 and 2.00 N - mg L^{-1} were prepared for each analysis.

3.2.3. DOM characterisation and concentration

A DOC-LABOR LC-OCD size-exclusion chromatography system (based on the Gräntzel thin-film UV-reactor), was used to identify concentrations of biopolymers (BP, molecular weight > 20,000 g mol^{-1}), humic substances (HS, 500 g mol^{-1} < molecular weight > 1000 g mol^{-1}), building blocks (BB, 300 g mol^{-1} < molecular weight > 500 g mol^{-1}), low molecular weight acids (LMWA, molecular weight < 350 g mol^{-1}), low molecular weight neutrals (LMWN, <350 g mol^{-1}) and hydrophobic organic carbon (HOC) in the samples. Chromatogram visualisation and peak position identification of each fraction described above is performed using a customised software program for LC-OCD output (ChromCALC, DOC-LABOR, Karlsruhe, Germany) developed by Huber et al. (2011). In summary, DOC fractions and molecular weights are determined based on compound retention times, using the dominating HS peak in the OCD chromatograms to identify the positioning of the other fractions. The position of the HS peak and molecular weight of the HS fraction has

been calibrated using International Humic Substance Society (IHSS) Suwannee River humic acid (HA) and fulvic acid (FA) standards (Huber et al., 2011). Further information regarding how LC-OCD fractions and molecular weights are classified and calculated can be found in Huber et al. (2011).

Solid phase extraction (SPE) onto reversed phase BondElut PPL sorbent (100 mg cartridges, Agilent Technologies) was performed prior to FT-ICR MS analysis using the methods described in Dittmar et al. (2008). Extracts were run at the National Magnetic Field Laboratory, Tallahassee, USA, using a negative mode (-) electrospray ionisation (ESI) on a 21 Tesla super conducting magnet (Bruker, U.S.) (Hendrickson et al., 2015; Smith et al., 2018). A modified aromaticity index (AI_{mod}) was calculated for molecular formula (Koch and Dittmar, 2016; Koch et al., 2007) in order to assess the degree of unsaturation. AI_{mod}, H/C ratios, O/C ratios and N were used to group neutral elemental compositions into compound classes. Polyphenolic compounds are defined as molecular formulae with $0.5 < AI_{mod} \leq 0.66$; condensed or polycyclic aromatic formulae are defined as $AI_{mod} > 0.66$; highly unsaturated and phenolic are defined as $AI_{mod} \leq 0.5$, H/C < 1.5, O/C $\leq$ 0.9; aliphatic formulae are defined as $1.5 \leq H/C \leq 2.0$, O/C $\leq$ 0.9 and N = 0; sugar-like formulae are defined as O/C > 0.9; and peptide-like formulae are defined as $1.5 \leq H/C \leq 2.0$, and N > 0 as per Kellerman et al. (2014). It is noted that these categories are based on atomic ratios derived from elemental compositions assigned in FT-ICR MS peaks and not indicative of structural classes of DOM compounds. Therefore, the term "group" does not refer to the compound structural motifs and refers to the range of atomic H/C and O/C ratios for each elemental composition assignment, discussed as percent relative abundance (% RA, scaled to the 100% peak within each spectrum) of a particular group in the sample.

The FT-ICR MS results represent only the SPE DOM within the analytical window present in FT-ICR MS. LC-OCD gives a lower resolution but entire view of the DOM spectrum, therefore both techniques have been used to gain a greater understanding of DOM in the samples. The unextracted DOM is chemically distinct from the extracted DOM, since composition controls part of extraction. This manuscript therefore uses FT-ICR MS data to explore the ways in which the extracted DOM differs between sites, whilst LC-OCD data is used to explore how bulk DOM differs between sites. The composition of the unextracted DOM is not explored.

Details of the methods used to perform statistical analyses, and further details of the limitations and representativeness of FT-ICR MS and LC-OCD data are presented in the Appendix.

4. RESULTS

The raw isotope, DOM characterisation, field data and inorganic anion results for all samples from Maules Creek, Wellington and Anna Bay are presented in Table S.1, Table S.2 and Table S.3, respectively. Information on the water types and sources identified is provided in the Appendix text and Fig. S.9, Fig. S.10 and Table S.4.

4.1. DOC age and concentration

Minimum and maximum $^{14}C_{DOC}$ values ranged from 72.9 ± 0.3 to 105.8 ± 0.3 pMC (Table 2) with the oldest sample at EC31 at Maules Creek (radiocarbon age = 2540 years before present (yBP)) which is a shallow regional groundwater sample (Table S.4).

The youngest $^{14}C_{DOC}$ values at Anna Bay were found in samples at the MLSs next to the wetland (MLSA_40cm, MLSB_100cm, MLSD_115cm, Table S.3). It is noted that due to problems with obtaining $^{14}C_{DOC}$ results for some samples with low DOC concentrations and high EC, $^{14}C_{DOC}$ results at Wellington were only available for Macquarie River, Bell River, and two bores influenced by Macquarie River water (WRS03 and WRS05). These samples were all classified as "modern" (Table S.2) and therefore younger than the radiocarbon reference year of 1950.

DOC concentrations in groundwater samples (i.e. excluding surface water samples) were highest at Anna Bay (average = 8.0 mg C L^{-1}, σ = 4.0, Table S.1–Table S.3). Both inland sites have low average and standard deviation groundwater DOC concentrations (average = 1.0, σ = 0.3 and average = 1.2 mg C L^{-1}, σ = 0.6 at Maules Creek and Wellington, respectively).

4.2. DOM character

At all sites, the dominant LC-OCD fraction is the HS fraction (500 g mol^{-1} < molecular weight > 1000 g mol^{-1}, Table 3). HS comprised an average of 60.3% ± 6.3 (1σ error) of DOM in Anna Bay samples, 56.6% ± 14 (1σ error) at Wellington, and 33.7% ± 11 (1σ error) at Maules Creek. LMWN (molecular weight < 350 g mol^{-1}) and HOC (classified as the material which does not leave the stationary phase in the column) were the next most dominant fractions with sample-averaged % RA of 9.8% ± 2.0 (1σ error) and 16.6% ± 6.4 (1σ error) respectively at Anna Bay, 18.2% ± 4.2 (1σ error) and 10.8 ± 10.1 (1σ error) respectively at Wellington, and 25.6% ± 7.9 (1σ error) and 24.9 ± 7.5 (1σ error) respectively at Maules Creek (Table 3 and Fig. S.11).

The most abundant FT-ICR MS compound class in the data across all sites corresponds to atomic ratios within the highly unsaturated and phenolic van Krevelen regions (Table 3). Compounds within the highly unsaturated and phenolic-like compositional groupings comprise an average of 72.7% ± 12.1 (1σ error) of DOM compounds detected in Anna Bay samples, 93.4% ± 3.7 (1σ error) at Wellington, and 95.6% ± 1.4 (1σ error) at Maules Creek, and were the most abundant groups across all sites. Polyphenolic and aliphatic compounds were second and third highest in relative abundance across all sites, with averages of 18.8% ± 8.6 (1σ error) and 2.9% ± 1.3 (1σ error) respectively at Anna Bay, 3.7% ± 2.4 (1σ error) and 2.3 ± 0.7 (1σ error) respectively at Wellington, and 2.6% ± 1.4 (1σ error) and 1.5% ± 0.4 (1σ error) respectively at Maules

Table 2
Summary of the average, median, minimum, maximum and standard deviation values for DOC concentration (mg L^{-1}), ^{14}C$_{DOC}$ (pMC), Δ^{14}C$_{DOC}$ (‰) and δ^{13}C$_{DOC}$ (‰) samples at Anna Bay (n = 8), Wellington (n = 7) and Maules Creek (n = 8).

		Average	Max	Median	Min	σ
DOC Concentration (mg L^{-1})	Anna Bay	8.0	15.1	7.4	1.0	4.0
	Wellington	2.3	8.3	1.6	0.6	2.7
	Maules Creek	1.0	1.3	1.1	0.6	0.3
^{14}C$_{DOC}$ (pMC)	Anna Bay	94.6	105.3	94.8	80.8	10.1
	Wellington	102.7	103.9	102.9	101.3	1.1
	Maules Creek	90.0	105.8	92.0	72.9	13.5
Δ^{14}C$_{DOC}$ (‰)	Anna Bay	−54.25	53.40	−52.25	−191.80	100.83
	Wellington	27.33	38.80	28.68	13.20	10.80
	Maules Creek	−99.97	57.7	−79.60	−270.90	135.47
^{13}C$_{DOC}$ (‰)	Anna Bay	−27.6	−26.7	−27.5	−28.5	0.8
	Wellington	−25.1	−23.9	−24.7	−26.4	1.0
	Maules Creek	−27.3	−23.2	−25.6	−36.1	4.7

Table 3
Summary of the percent relative abundance (% RA) of FT-ICR MS and LC-OCD groups at each site. LC-OCD groupings include biopolymers (BP, molecular weight > 20,000 g mol^{-1}), humic substances (HS, 500 g mol^{-1} < molecular weight > 1000 g mol^{-1}), building blocks (BB, 300 g mol^{-1} < molecular weight > 500 g mol^{-1}), low molecular weight neutrals (LMWN, <350 g mol^{-1}) and hydrophobic organic carbon (HOC, defined as the fraction that does not leave the LC-OCD column). FT-ICR MS groupings include polyphenolic compounds (0.5 < AI$_{mod}$ ≤ 0.66), condensed aromatic formulae (AI$_{mod}$ > 0.66), highly unsaturated and phenolic (AI$_{mod}$ ≤ 0.5, H/C < 1.5, O/C ≤ 0.9), aliphatic formulae (1.5 ≤ H/C ≤ 2.0, O/C ≤ 0.9 and N = 0), sugar-like formulae (O/C > 0.9); and peptide-like formulae (1.5 ≤ H/C ≤ 2.0, and N > 0). FT-ICR MS data also shows the average % RA of CHO, CHON, CHONS and CHOS containing groups.

Group	Average % RA ± 1σ error (Maules Creek)	Average % RA ± 1σ error (Wellington)	Average % RA ± 1σ error (Anna Bay)
LCOCD			
HOC	24.9 ± 7.5	10.8 ± 10.1	16.6 ± 6.4
BP	1.3 ± 2.5	1.6 ± 1.8	0.3 ± 0.3
HS	33.7 ± 14.0	56.6 ± 11.0	60.3 ± 6.3
BB	14.5 ± 6.0	12.8 ± 5.2	13.0 ± 2.0
LMWN	25.6 ± 7.9	18.2 ± 4.2	9.8 ± 2.1
FT-ICR MS			
Peptide-like	0.1 ± 0.0	0.1 ± 0.1	0.1 ± 0.1
Sugar-like	0.0 ± 0.0	0.0 ± 0.1	0.1 ± 0.1
Condensed Aromatics	0.2 ± 0.3	0.5 ± 0.8	5.6 ± 5.1
Polyphenolic	2.6 ± 1.4	3.7 ± 2.4	18.8 ± 8.6
Highly Unsaturated and Phenolic	95.6 ± 1.4	93.4 ± 3.7	72.7 ± 12.1
Aliphatic	1.5 ± 0.4	2.3 ± 0.7	2.9 ± 1.3
CHO	89.2 ± 2.8	83.5 ± 2.9	84.3 ± 2.9
CHON	9.2 ± 2.3	13.0 ± 3.3	6.4 ± 1.0
CHONS	0.0 ± 0.1	0.1 ± 0.2	0.0 ± 0.1
CHOS	1.6 ± 0.7	3.4 ± 1.0	9.3 ± 3.0

Creek (Table 3). Notably, the highly unsaturated and phenolic group at Maules Creek and Wellington are comprised of much lower O/C ratios compared to Anna Bay (Fig. 2).

In terms of compound composition, CHO compounds were the most abundant at all sites (89.2% ± 2.8, 83.5% ± 2.9 and 84.3% ± 2.9 at Maules Creek, Wellington and Anna Bay, respectively). Anna Bay samples are observed to contain slightly higher CHOS molecular formulae (9.3% ± 3.0) compared to Maules Creek (1.6% ± 0.7) and Wellington (3.4% ± 1.0). The presence or absence of N or S are not correlated with ^{14}C$_{DOC}$ age for either the inland or the coastal site (p > 0.1 for all Spearman's rank correlation coefficients).

4.3. Abundances of molecular formulae

In total, 15,790 unique elemental compositions were derived from negative-ion ESI FT-ICR MS across 23 samples. Wellington samples were the most compositionally complex, with the highest number of elemental compositions assigned, followed by Anna Bay and Maules Creek (Table 4). 95% of compositional diversity was reached in
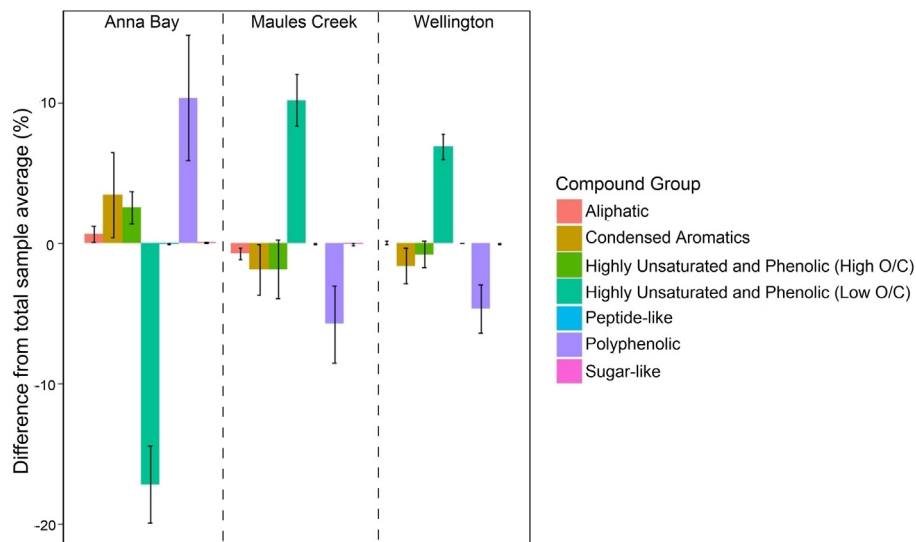
Fig. 2. Percent deviation for site average relative abundance (% RA) of each compound group compared to the total sample average at all sites (normalised to 0) with error bars (1 σ). Highly unsaturated and phenolics are shown separated into high (O/C > 0.5) and low (O/C < 0.5) oxygen categories based on atomic O/C ratios derived from (-)ESI FT-ICR MS.

Table 4
Summary of the total number of individual DOM elemental composition assignments at each site, the number of unique elemental compositions assigned at each site, and the average number of elemental compositions identified per sample at each site.

	Total number of elemental compositions assigned (all samples)	Number of unique elemental compositions	Average number of elemental compositions per sample
Anna Bay (n = 8)	11,702	2,792	7,331
Wellington (n = 7)	11,954	1,115	7,343
Maules Creek (n = 8)	10,123	535	6,093

17 of 23 samples (i.e. 74% of samples) which indicates that the elemental compositions derived were not consistent between samples (Fig. S.12).

Maules Creek had the lowest number of molecular formulae unique to the study site. Wellington and Anna Bay had the largest average number of assignments per sample with a two-tailed t-test showing no significant differences between Wellington and Anna Bay sites (p = 0.99). The average number of total elemental compositions per sample at Maules Creek (6093) was significantly lower than both Wellington (7343) and Anna Bay (7331, p = < 0.05). Surface or near-surface water samples correspond to the samples with the highest number of elemental composition assignments. These included Macquarie River (n = 8989) at Wellington, MLSA_40cm (n = 8862) at Anna Bay and surface water (n = 7450) at Maules Creek.

4.4. Molecular composition of DOM with $^{14}C_{DOC}$ age

At Anna Bay, the sample with the oldest $^{14}C_{DOC}$ value is at S4_S (80.82 pMC), with a conventional radiocarbon age of 1710 ± 30 yBP. This sample is located furthest from the wetland, and contains a higher relative abundance of condensed aromatics and polyphenolic (17.0% RA and 34.6%

RA, respectively) compounds compared to the average for Anna Bay (5.6% RA and 18.8% RA, respectively). Research has shown that aromatic DOM is susceptible to photodegradation (Stubbins et al., 2010) and sorption to mineral surfaces (Jardine et al., 1989; Kaiser et al., 1996), which suggests that this sample has not been exposed to photodegradation or sorption mechanisms. The sample also contains a low weighted average H/C ratio of 0.86 which is the minimum found in any sample at Anna Bay (Table S.3). High ^3H levels in this sample compared to the regional groundwater samples, and low EC compared to the samples close to the wetland, suggests that the water has been recently exposed to the atmosphere and has not had time to incorporate many dissolved ions from weathering or evaporation. This suggests that the water source probably comes from recent diffuse recharge (Table S.4), with aged DOC leached from a peat layer at the site. At Maules Creek the sample with the oldest $^{14}C_{DOC}$ value was located at Elfin Crossing in the shallow regional groundwater at EC31 (71.91 pMC) closely followed by the deep regional groundwater sample BH12-4 (75.22 pMC). These samples have conventional radiocarbon ages of 2540 ± 40 yBP and 2285 ± 40 yBP respectively. When compared to the aged DOM samples from Anna Bay, these

samples contain low % RA condensed aromatics and polyphenolic and a large % RA of highly unsaturated and phenolic compounds.

The samples with the youngest $^{14}C_{DOC}$ values were located at the wetland at Anna Bay (MLSA, 105.3 pMC), BH18-2 at Maules Creek (105.8 pMC), and at Macquarie River in Wellington (103.9 pMC, 38.8 ‰). BH18-2 and Macquarie River have the highest % RA condensed aromatics and polyphenolic of all samples at the respective sampling sites in Maules Creek and Wellington. The MLS piezometers at Anna Bay had similar FT-ICR MS compound group % RA distribution to the Macquarie River sample, however due to the high % RA of condensed aromatics and polyphenolic in the peat-derived DOM samples, the MLS samples had the lowest % RA of condensed aromatics and polyphenolic for the Anna Bay site. This is reflected in Fig. 3 which shows aromatic compounds are not significantly correlated with younger DOM, instead, aromatic compounds are significantly correlated with aged DOM at Anna Bay. In contrast, at Wellington and Maules Creek, aromatic regions of the van Krevelen diagram are not significantly correlated with aged DOM and there are no molecular formulae significantly correlated with younger DOC at these sites. The two distinctly different regions of aged DOM at the Anna Bay and Wellington/ Maules Creek sites, and the region of young DOM at the Anna Bay site shown in Fig. 3 indicate three potential DOM end-members which are explored further in the following sections.

4.5. Compositional end-members of groundwater DOM

Principal component analysis (Fig. 4) using DOM variables including LC-OCD fractions (% RA), FT-ICR MS groups (% RA), $^{14}C_{DOC}$ (pMC), $\delta^{13}C_{DOC}$ (‰) and DOC concentration (mg C L^{-1}) shows that the data at the sites

group between three end-members which all have unique DOM compositions and characteristics on the x and y-axes (Fig. 4A). This supports the results of the Spearman correlations shown in Fig. 3. The three DOM end-members identified include aged peat DOM, a young terrestrial DOM source and an aged DOM by-product (Fig. 4A). Further discussion regarding the end-member water and DOM sources is provided in the Appendix.

Anna Bay samples are distributed to the left on the PCA biplot (Fig. 4A) between the aged sedimentary peat end-member sample (S4_S) on the lower y-axis, and a young terrestrial surface DOM end-member (MLSA_40cm and MLSB_100cm) on the upper y-axis. Fig. 4A shows that S4_S is the cleanest peat DOM sample of the entire cohort and this is supported by EC and ^3H data (Table S.3) which indicates the water is diffuse recharge source and is therefore least likely to be mixed with DOM from other sources. The sedimentary peat DOM signal is identified by high DOC concentrations, and high % RA of HS, polyphenolic and condensed aromatics on PC1 (Fig. 4B). It is characterised by low $^{14}C_{DOC}$ (pMC) and aliphatics, and high HOC on PC2 (Fig. 4C).

The young terrestrial surface water DOM source is differentiated from the aged DOM by variables influencing PC2 on the y-axis. These include high $^{14}C_{DOC}$ pMC values and high % RA aliphatics and peptide-like DOM. These characteristics of young terrestrial DOM are consistent in both Anna Bay wetland samples and Wellington river samples.

The aged, stable by-product end-member is identified at the inland samples at Wellington (shown in blue font on Fig. 4) and Maules Creek (shown in green font on Fig. 4). This by-product DOM is characterised by high % RA highly unsaturated and phenolics, HOC and LMWN, and low % RA polyphenolic, HS and DOC concentration on PC1. On PC2 it is characterised by low $^{14}C_{DOC}$ (pMC)
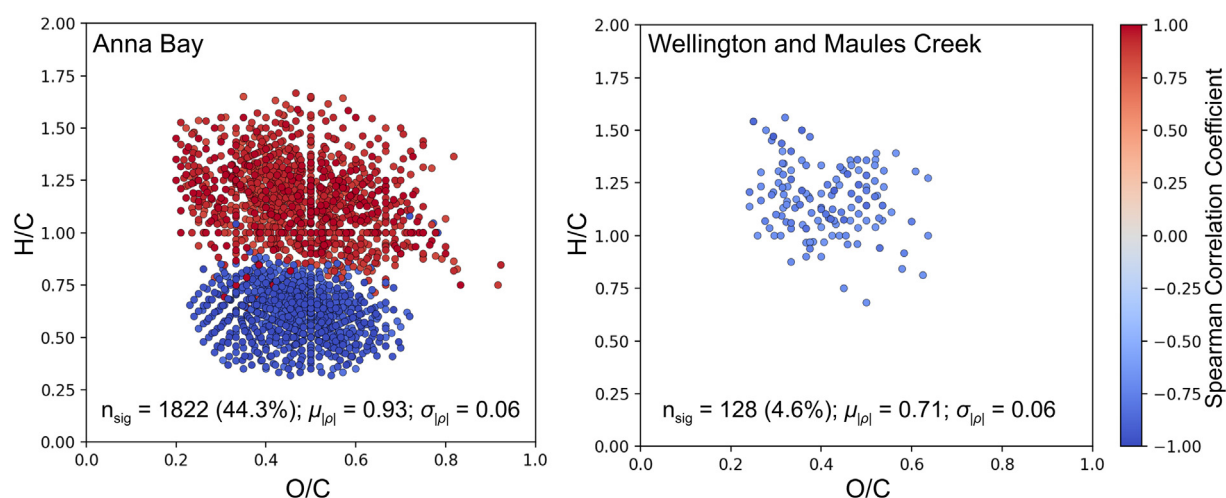

Fig. 3. Spearman correlations of individual molecular formulae that are significantly correlated with $^{14}C_{DOC}$ age (pMC) at Anna Bay (left), and Wellington and Maules Creek (right). Blue dots represent formulae that are significantly negatively correlated with $^{14}C_{DOC}$ pMC (i.e. formulae consistent with aged DOM). Red dots represent formulae that are significantly positively correlated with $^{14}C_{DOC}$ pMC (i.e. formulae consistent with young DOM). (For interpretation of the references to colour in this figure legend, the reader is referred to the web version of this article.)
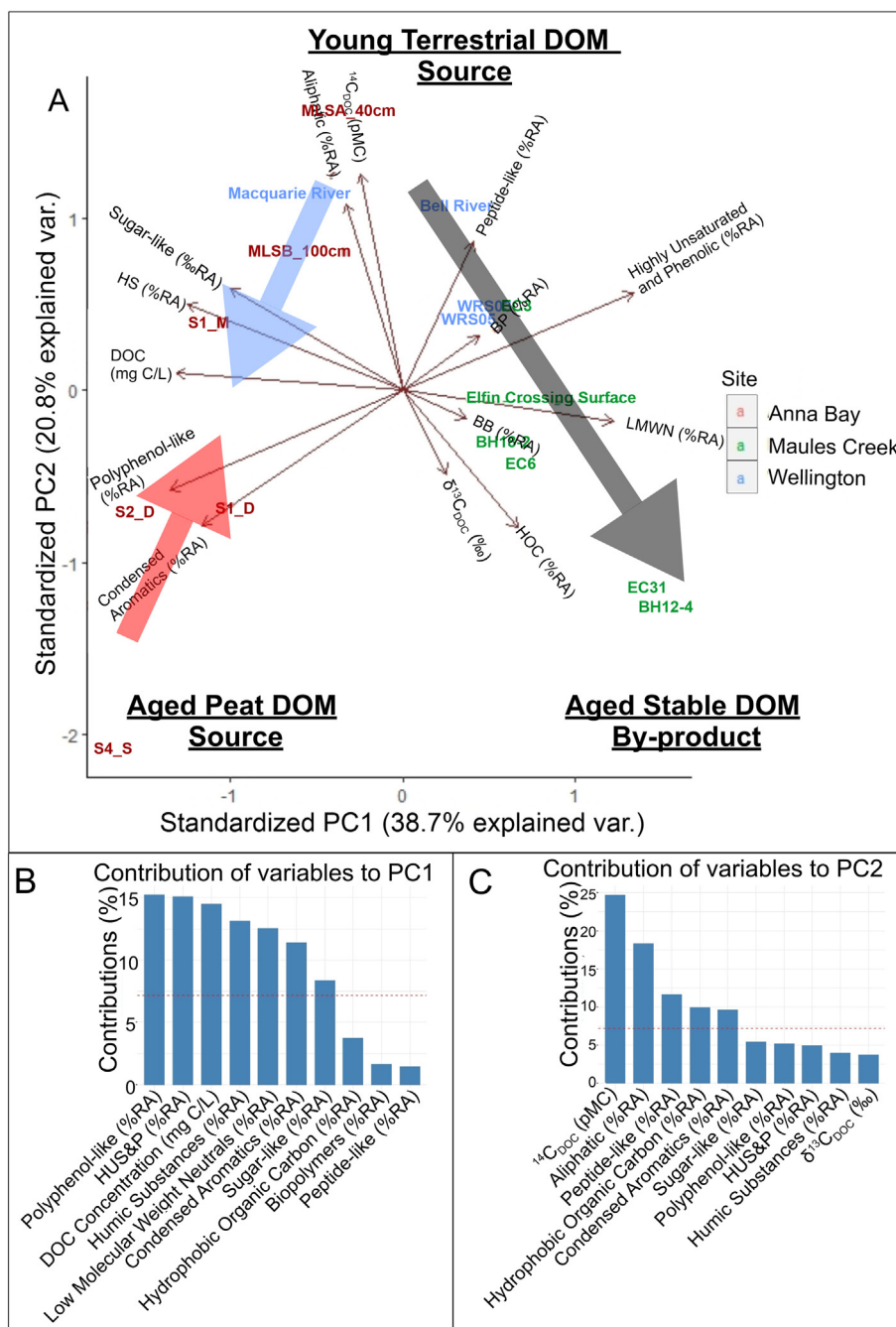
Fig. 4. (A) PCA of samples using DOM variables ($^{14}C_{DOC}$ (pMC), $\delta^{13}C_{DOC}$ (‰), DOC concentration (mg C L^{-1}), LC-OCD fractions (% RA) and FT-ICR MS groups (% RA). The analysis shows clear groupings of Anna Bay samples (red font), Maules Creek samples (green font) and Wellington samples (blue font). The coastal Anna Bay samples are differentiated from the inland samples by variables explaining PC1 (shown in B). At Anna Bay, the PCA identifies a mix of two DOM end-members (aged peat DOM and young terrestrial DOM). These are distinguished by PC2 variables (shown in C) with the mixing of these sources at Anna Bay represented by the red and blue arrows. Maules Creek and Wellington samples comprise a mix of young terrestrial DOM which ages into stable by-product DOM which are also distinguished by PC2 variables. The degradation into stable DOM at the inland sites is represented by the grey arrow. NB: samples without a result for $^{14}C_{DOC}$ have not been included. Highly unsaturated and phenolics is abbreviated as HUS&P in the lower bar charts. (For interpretation of the references to colour in this figure legend, the reader is referred to the web version of this article.)

and low % RA aliphatics. It is noted that whilst the transformation pathway from surface water DOM to stable by-product DOM shown in Fig. 4 is likely to be applicable to other shallow groundwater environments where there is no other significant input of DOM, the change in DOM composition with age may differ in larger regional groundwater systems, especially where hydrocarbon deposits may be present.

There is a significant positive correlation between $^{14}C_{DOC}$ (pMC) and DOC concentration at the inland sites (p = 0.04, Spearman's rho (r_s) = 0.66) which is not seen at the coastal site (p = 1.00, r_s = −0.03, Table S.5). This indicates that at Anna Bay, the input of unprocessed aged DOM is overwhelming any processed DOM signal. At Maules Creek and Wellington, the positive relationship between $^{14}C_{DOC}$ (pMC) and DOC concentration indicate that DOC is processed and removed over time. Maules Creek is observed as having the lowest number of unique molecular formulae, and is largely comprised of the same molecular formulae present at the other sites. This further supports the hypothesis that groundwater DOM at this site is highly processed with stable DOM remaining.

5. DISCUSSION

5.1. Groundwater DOM sources and processing pathways

Two sources of DOM in groundwater were identified, including a DOM source originating from surface waters, and DOM originating from sedimentary organic matter in the subsurface (Fig. 4). An aged and stable by-product DOM was also identified. The results show that unprocessed sedimentary OM-derived DOM at Anna Bay is associated with high O/C ratios, low H/C ratios, high molecular weight, high aromaticity DOM with a large % RA of HS and polyphenolics. In contrast, processed groundwater DOM in the inland sites is associated with lower O/C ratios, higher H/C ratios and a greater proportion of LMWN, which are likely to include microbial metabolites (Shen et al. 2015). These finding support the size-reactivity continuum model for OM decomposition in aquatic environments proposed by Amon and Benner (1996) who suggest an overall processing of high molecular weight DOM to low molecular weight DOM over time. Our finding of a greater proportion of aliphatic and peptide-like DOM compounds in the young terrestrial DOM suggests that this source is more biolabile (Hopkinson et al., 1998) whilst the aged sedimentary peat source may be vulnerable to photodegradation or adsorption to mineral surfaces due to its high molecular weight and aromaticity (Jardine et al., 1989; Kaiser et al., 1996; Stubbins et al., 2010; Shen et al., 2015) when transported along a subsurface flow path and discharged to a surface environment. Compounds with higher DBE, higher O/C and lower H/C ratios, as is observed with the sedimentary peat source, are more susceptible to adsorption (Coward et al., 2018). The greater proportion of highly unsaturated and phenolic low O/C molecular formulae at inland sites (refer to Fig. 2) suggests that DOM with high O/C ratios is processed out along pathways due to adsorption or degradation. As an example, this is supported by a clear removal of the high O/C and low H/C ratio DOM present in Macquarie River as it is recharging the aquifer at WRS03 (Fig. S.13). Fig. S.14 also shows a significant decrease in O/C ratios and increase in H/C ratios with increased screen depth at the inland sites (both p < 0.01) suggesting increased DOM adsorption with depth.

Huber et al. (2011) define a humification pathway of surface waters based on HS aromaticity and HS nominal average molecular weight as measured by LC-OCD analysis using IHSS standards and a range of European surface water samples. The surface water samples analysed in this study (Macquarie River, Bell River and Elfin Crossing) have 54.4% ± 33 (n = 3) lower molecular weight compared to the surface water samples presented in the HS diagram of Huber et al. (2011) (n = 20). This may be a result of the high levels of UV irradiation these surface waters receive in Australia, and associated photodegradation (Osburn et al., 2001). Processed groundwater samples from this research (Maules Creek and Wellington) display reduced average HS aromaticity (defined as the spectral absorption coefficient/organic carbon in litres per milligram per meter) (1.28 ± 0.43, n = 12) compared to the surface water samples from Wellington and Maules Creek (2.72 ± 0.68, n = 3), without further reduction in molecular weight. This indicates that subsurface DOM processing mechanisms such as adsorption and biodegradation largely impact HS aromaticity.

5.2. Groundwater DOM preservation mechanisms

Radiocarbon dating is not frequently undertaken when assessing DOM in aqueous environments, however this research shows that $^{14}C_{DOC}$ analyses combined with DOM characterisation techniques can assist in identifying carbon sources as well as the transformation of DOM as it is processed. The combination of these techniques can also provide insights into the preservation mechanisms of DOM in surface waters and groundwater. Recent research indicates that DOC is preserved in surface waters and marine and soil sediment via two mechanisms; selective preservation of compounds that are intrinsically stable (non-biolabile and therefore not able to be microbially processed), and protection from degradation by mineral interaction where particles are shielded from biological respiration (Hemingway et al., 2019). Hemingway et al. (2019) propose that the selective preservation mechanism would result in a decline in DOM diversity (determined by the distribution of C bond strengths), whilst the mineral interaction/protection mechanism results in an increase in DOM diversity. Despite the semi-quantitative nature of FT-ICR MS data, previous studies have used FT-ICR MS in quantitative statistical analyses (Flerus et al., 2012; Seidel et al. (2017); Poulin et al., 2017). In this context, the number of molecular formulae assigned shows a weak statistically significant positive linear relationship between aging DOM (declining $^{14}C_{DOC}$ (pMC)) and declining DOM diversity (p = 0.04, using number of unique molecular formulae as a proxy for bond strength diversity, Fig. S.15). We note that the relationship is not present at all sites and appears to be strongest at Anna Bay, which suggests that the relative percentage of sedimentary OM may also be an important control on groundwater DOM diversity.

6. CONCLUSIONS

Our research combines FT-ICR MS, LC-OCD and isotopic techniques for the first time to determine groundwater DOM sources, end-members, and molecular composition in

contrasting hydrogeological contexts. Inorganic chemistry, $^{14}C_{DIC}$ and ^3H were used to identify water sources, with $^{14}C_{DOC}$, DOM characterisation and PCA used to identify DOM sources and processing pathways. We identified the character of two unique DOM source inputs. A young terrestrial surface DOM source is identified and shares a similar composition regardless of site, and was characterised by higher % RA peptide-like and aliphatic compounds compared to the other end-members. The character of aged DOM varied between sites and was differentiated from young fresh terrestrial DOM by its molecular composition. Spearman correlations uncovered the molecular character of an aromatic aged sedimentary peat DOM source with high % RA polyphenolic, condensed aromatics and HS at Anna Bay. In addition, we identify the change in DOM composition in two semi-arid environments as it is processed into a stable by-product DOM. The processing of groundwater DOM in semi-arid environments is characterised by an increasing % RA of LMWN and highly unsaturated and phenolic compounds, and decreasing % RA of aliphatics, peptide-like, polyphenolic and condensed aromatic DOM, which we suggest is a result of biodegradation, adsorption and limited leaching of fresh terrestrial or sedimentary DOM due to the dry and aged landscapes that these sites represent. We observe an increase in DOM H/C ratios and decline in O/C ratios with groundwater DOM processing which suggests that adsorption is a major removal pathway in aquifers. These results show that the composition of aged groundwater DOM can differ between temperate coastal sites and semi-arid inland sites due to high or low inputs of sedimentary OM and confirm our hypotheses that DOM source and DOM age both contribute to the composition of aged DOC, with the stable by-product DOM signal overwhelmed in locations of high sedimentary OM inputs.

APPENDIX A. SUPPLEMENTARY MATERIAL

Supplementary data to this article can be found online at https://doi.org/10.1016/j.gca.2020.01.022.

REFERENCES

Amon R. M. W. and Benner R. (1996) Bacterial utilization of different size classes of dissolved organic matter. *Limnol. Oceanogr.* **41**, 41–51.

Andersen M. S. and Acworth R. I. (2009) Stream-aquifer interactions in the Maules Creek catchment, Namoi Valley, New South Wales, Australia. *Hydrogeol. J.* **17**, 2005–2021.

Appelo C. and Postma D. (2005) *Geochemistry, Groundwater and Pollution*, second ed. Balkema, Rotterdam.

Assayag N., Rivé K., Ader M., Jézéquel D. and Agrinier P. (2006) Improved method for isotopic and quantitative analysis of dissolved inorganic carbon in natural water samples. *Rapid Commun. Mass Spectrom.* **20**, 2243–2251.

Banwart S. A. (1999) Reduction of iron(III) minerals by natural organic matter in groundwater. *Geochim. Cosmochim. Acta* **63**, 2919–2928.

Battin T. J., Luyssaert S., Kaplan L. A., Aufdenkampe A. K., Richter A. and Tranvik L. J. (2009) The boundless carbon cycle. *Nat. Geosci.* **2**, 598–600.

Barnes R. T., Butman D. E., Wilson H. F. and Raymond P. A. (2018) Riverine export of aged carbon driven by flow path depth and residence time. *Environ. Sci. Technol.* **52**, 1028–1035.

Bryan E., Meredith K. T., Baker A., Andersen M. S. and Post V. E. A. (2017) Carbon dynamics in a Late Quaternary-age coastal limestone aquifer system undergoing saltwater intrusion. *Sci. Total Environ.* **607–608**, 771–785.

Burrows R. M., Rutlidge H., Bond N., Eberhard S., Auhl A., Andersen M. S., Valdez D. and Kennard M. (2017) High rates of organic carbon processing in the hyporheic zone of intermittent streams. *Sci. Rep.* **7**, 1–11.

Burrows R. M., Rutlidge H., Valdez D., Vernarsky M., Bond N., Andersen M. S., Fry B., Eberhard S. and Kennard M. J. (2018) Groundwater supports intermittent stream food webs. *Freshw. Science* **37**, 42–53.

Catalán N., Marcé R., Kothawala D. N. and Tranvik L. J. (2016) Organic carbon decomposition rates controlled by water retention time across inland waters. *Nat. Geosci.* **9**, 501.

Coward E. K., Ohno T. and Plante A. F. (2018) Adsorption and molecular fractionation of dissolved organic matter on iron-bearing mineral matrices of varying crystallinity. *Environ. Sci. Technol.* **52**, 1036–1044.

Dittmar T., Koch B., Hertkorn N. and Kattner G. (2008) A simple and efficient method for the solid-phase extraction of dissolved organic matter (SPE-DOM) from seawater. *Limnol. Oceanogr. Meth.* **6**, 230–235.

Evans S., Campbell C. and Naidenko O. V. (2019) Cumulative risk analysis of carcinogenic contaminants in United States drinking water. *Heliyon* **5** e02314.

Feng L., An Y., Xu J. and Kang S. (2018) Characteristics and sources of dissolved organic matter in a glacier in the northern Tibetan Plateau: differences between different snow categories. *Ann. Glaciol.* **59**, 31–40.

Flerus R., Lechtenfeld O. J., Koch B. P., McCallister S. L., Schmitt-Kopplin P., Benner R., Kaiser K. and Kattner G. (2012) A molecular perspective on the ageing of marine dissolved organic matter. *Biogeosciences* **9**, 1935–1955.

Giambastiani B. M. S., McCallum A. M., Andersen M. S., Kelly B. F. J. and Acworth R. I. (2012) Understanding groundwater processes by representing aquifer heterogeneity in the Maules Creek Catchment, Namoi Valley (New South Wales, Australia). *Hydrogeol. J.* **20**, 1027–1044.

Grannas A. M., Hockaday W. C., Hatcher P. G., Thompson L. G. and Mosley-Thompson E. (2006) New revelations on the nature of organic matter in ice cores. *J. Geophys. Res.* **111**(D4), D04304.

Hemingway J. D., Rothman D. H., Grant K. E., Rosengard S. Z., Eglinton T. I., Derry L. A. and Galy V. V. (2019) Mineral protection regulates long-term global preservation of natural organic carbon. *Nature* **570**, 228–231.

Hendrickson C. L., Quinn J. P., Kaiser N. K., Smith D. F., Blakney G. T., Chen T., Marshall A. G., Weisbrod C. R. and Beu S. C. (2015) 21 tesla fourier transform ion cyclotron resonance mass spectrometer: a national resource for ultrahigh resolution mass analysis. *J. Am. Soc. Mass Spectrom.* **26**, 1626–1632.

Hertkorn N., Benner R., Frommberger M., Schmitt-Kopplin P., Witt M., Kaiser K., Kettrup A. and Hedges J. I. (2006) Characterization of a major refractory component of marine dissolved organic matter. *Geochim. Cosmochim. Acta* **70**, 2990–3010.

Hopkinson C. S., Buffam I., Hobbie J., Vallino J., Perdue M., Eversmeyer B., Prahl F., Covert J., Hodson R., Moran M., Smith E., Baross J., Crump B., Findlay S. and Foreman K. (1998) Terrestrial inputs of organic matter to coastal ecosystems: an intercomparison of chemical characteristics and bioavailability. *Biogeochemistry* **43**, 211–234.

Hua Q., Jacobsen G. E., Zoppi U., Lawson E. M., Williams A. A., Smith A. M. and McGann M. J. (2001) Progress in radiocarbon target preparation at the ANTARES AMS centre. *Radiocarbon* **43**, 275–282.

Huber S. A., Balz A., Abert M. and Pronk W. (2011) Characterisation of aquatic humic and non-humic matter with size-exclusion chromatography – organic carbon detection – organic nitrogen detection (LC-OCD-OND). *Water Res.* **45**, 879–885.

Jardine P. M., McCarthy J. F. and Weber N. L. (1989) Mechanisms of dissolved organic carbon adsorption on soil. *Soil Sci. Soc. Am. J.* **53**, 1378–1385.

Johannesson K. H., Yang N., Trahan A. S., Telfeyan K., Jade Mohajerin T., Adebayo S. B., Akintomide O. A., Chevis D. A., Datta S. and White C. D. (2019) Biogeochemical and reactive transport modeling of arsenic in groundwaters from the Mississippi River delta plain: An analog for the As-affected aquifers of South and Southeast Asia. *Geochim. Cosmochim. Acta* **264**, 245–272.

Johnson B. D. (1975) The Garra Formation (early Devonian) at Wellington, N.S.W. *J. proc. R. Soc. N.S.W.* **108**, 111–118.

Kaiser K., Canedo-Oropeza M., McMahon R. and Amon R. M. W. (2017) Origins and transformations of dissolved organic matter in large Arctic rivers. *Sci. Rep.* **7**, 13064.

Kaiser K., Guggenberger G. and Zech W. (1996) Sorption of DOM and DOM fractions to forest soils. *Geoderma* **74**, 281–303.

Kaiser K. and Kalbitz K. (2012) Cycling downwards – dissolved organic matter in soils. *Soil Biol. Biochem.* **52**, 29–32.

Kellerman A. M., Dittmar T., Kothawala D. N. and Tranvik L. J. (2014) Chemodiversity of dissolved organic matter in lakes driven by climate and hydrology. *Nat. Commun.* **5**, 3804.

Kellerman A. M., Guillemette F., Podgorski D. C., Aiken G. R., Butler K. D. and Spencer R. G. M. (2018) Unifying concepts linking dissolved organic matter composition to persistence in aquatic ecosystems. *Environ. Sci. Technol.* **52**, 2538.

Kellerman A. M., Kothawala D. N., Dittmar T. and Tranvik L. J. (2015) Persistence of dissolved organic matter in lakes related to its molecular characteristics. *Nat. Geosci.* **8**, 454–457.

King E. K., Perakis S. S. and Pett-Ridge J. C. (2018) Molybdenum isotope fractionation during adsorption to organic matter. *Geochim. Cosmochim. Acta* **222**, 584–598.

Koch B. P. and Dittmar T. (2016) From mass to structure: an aromaticity index for high-resolution mass data of natural organic matter. *Rapid Commun. Mass Spectrom.* **30**, 250 250.

Koch B. P., Dittmar T., Witt M. and Kattner G. (2007) Fundamentals of molecular formula assignment to ultrahigh resolution mass data of natural organic matter. *Anal. Chem.* **79**, 1758–1763.

Lechleitner F. A., Dittmar T., Baldini J. U. L., Prufer K. M. and Eglinton T. I. (2017) Molecular signatures of dissolved organic matter in a tropical karst system. *Org. Geochem.* **113**, 141–149.

Lechtenfeld O. J., Kattner G., Flerus R., McCallister S. L., Schmitt-Kopplin P. and Koch B. P. (2014) Molecular transformation and degradation of refractory dissolved organic matter in the Atlantic and Southern Ocean. *Geochim. Cosmochim. Acta* **126**, 321–337.

Li X., Tang C., Cao Y. and Li X. (2019) Carbon, nitrogen and sulfur isotopic features and the associated geochemical processes in a coastal aquifer system of the Pearl River Delta, China. *J. Hydrol.* **575**, 986–998.

Lis G., Wassenaar L. and Hendry M. (2008) High-precision laser spectroscopy D/H and $^{18}O/^{16}O$ measurements of microliter natural water samples. *Anal. Chem.* **80**, 287.

Longnecker K. and Kujawinski E. B. (2011) Composition of dissolved organic matter in groundwater. *Geochim. Cosmochim. Acta* **75**, 2752–2761.

McCallum A. M., Andersen M. S., Giambastiani B. M. S., Kelly B. F. J. and Acworth R. I. (2013) River–aquifer interactions in a semi-arid environment stressed by groundwater abstraction. *Hydrol. Process.* **27**, 1072–1085.

McDonough L. K., O'Carroll D. M., Meredith K., Andersen M. S., Brügger C., Huang H., Rutlidge H., Behnke M., Spencer R. G. M., McKenna A., Marjo C. E., Oudone P. and Baker A. (2020) Changes in groundwater dissolved organic matter character in a coastal sand aquifer due to rainfall recharge. *Water Res.* **169** 115201.

Meredith K. T., Baker A., Andersen M. S., O'Carroll D. M., Rutlidge H., McDonough L. K., Oudone P., Bryan E. and Zainuddin N. S. (2019) Isotopic and chromatographic fingerprinting of the sources of dissolved organic carbon in a shallow coastal aquifer. *Hydrol. Earth Syst. Sci. Discuss.* **2019**, 1–20. https://doi.org/10.5194/hess-2018-627.

O'Donnell J. A., Aiken G. R., Butler K. D., Guillemette F., Podgorski D. C. and Spencer R. G. (2016) DOM composition and transformation in boreal forest soils: the effects of temperature and organic-horizon decomposition state. *J. Geophys. Res. Biogeo.* **121**, 2727–2744.

Osburn C. L., Morris D. P., Thorn K. A. and Moeller R. E. (2001) Chemical and optical changes in freshwater dissolved organic matter exposed to solar radiation. *Biogeochemistry* **54**, 251–278.

Plummer L. N. and Glynn P. D. (2013) Radiocarbon dating in groundwater systems. In *Isotope Methods for Dating Old Ground-*

. International Atomic Energy Agency (IAEA), Vienna, pp. 33–89.

Poulin B. A., Ryan J. N., Nagy K. L., Stubbins A., Dittmar T., Orem W., Krabbenhoft D. P. and Aiken G. R. (2017) Spatial dependence of reduced sulfur in everglades dissolved organic matter controlled by sulfate enrichment. *Environ. Sci. Technol.* **51**, 3630–3639.

Raymond P. A. and Bauer J. E. (2001) Use of ^{14}C and ^{13}C natural abundances for evaluating riverine, estuarine, and coastal DOC and POC sources and cycling: a review and synthesis. *Org. Geochem.* **32**, 469–485.

Reemtsma T., These A., Linscheid M., Leenheer J. and Spitzy A. (2008) Molecular and structural characterization of dissolved organic matter from the deep ocean by FTICR-MS, including hydrophilic nitrogenous organic molecules. *Environ. Sci. Technol.* **42**, 1430–1437.

Schiff S. L., Aravena R., Trumbore S. E. and Dillon P. J. (1990) Dissolved organic carbon cycling in forested watersheds: a carbon isotope approach. *Water Resour. Res.* **26**, 2949–2957.

Seidel M., Manecki M., Herlemann D. P. R., Deutsch B., Schulz-Bull D., Jürgens K. and Dittmar T. (2017) Composition and transformation of dissolved organic matter in the Baltic Sea. *Front. Earth Sci.* **5**, 1–20.

Shen Y., Chapelle F. H., Strom E. W. and Benner R. (2015) Origins and bioavailability of dissolved organic matter in groundwater. *Biogeochemistry* **122**, 61–78.

Sickman J. O., DiGiorgio C. L., Davisson M. L., Lucero D. M. and Bergamaschi B. (2010) Identifying sources of dissolved organic carbon in agriculturally dominated rivers using radiocarbon age dating: Sacramento-San Joaquin River Basin, California. *Biogeochemistry* **99**, 79–96.

Smith D. F., Podgorski D. C., Rodgers R. P., Blakney G. T. and Hendrickson C. L. (2018) 21 tesla FT-ICR mass spectrometer for ultrahigh-resolution analysis of complex organic Mixtures. *Anal. Chem.* **90**, 2041–2047.

Spencer R. G. M., Guo W., Raymind P. A., Dittmar T., Hood E., Fellman J. and Stubbins A. (2014) Source and biolability of ancient dissolved organic matter in glacier and lake ecosystems on the Tibetan Plateau. *Geochim. Cosmochim. Acta* **142**, 64–74.

Spencer R. G. M., Mann P. J., Dittmar T., Eglinton T. I., McIntyre C., Holmes R. M., Zimov N. and Stubbins A. (2015) Detecting the signature of permafrost thaw in Arctic rivers. *Geophys. Res. Lett.* **42**, 2830–2835.

Stubbins A., Spencer R., Chen H. M., Hatcher P. G., Mopper K., Hernes P., Mwamba V., Mangangu A., Wabakanghanzi J. and Six J. (2010) Illuminated darkness: molecular signatures of Congo River dissolved organic matter and its photochemical alteration as revealed by ultrahigh precision mass spectrometry. *Limnol. Oceanogr.* **55**, 1467–1477.

Stuiver M. and Polach H. A. (1977) Discussion reporting of 14C data. *Radiocarbon* **19**, 355–363.

Textor S. R., Wickland K. P., Podgorski D. C., Johnston S. E. and Spencer R. G. M. (2019) Dissolved organic carbon turnover in permafrost-influenced watersheds of interior alaska: molecular insights and the priming effect. *Front. Earth Sci.* **7**, 1–17.

Wang Y., Spencer R. G., Podgorski D. C., Kellerman A. M., Rashid H., Zito P., Xiao W., Wei D., Yang Y. and Xu Y. (2018) Spatiotemporal transformation of dissolved organic matter along an alpine stream flow path on the Qinghai-Tibet Plateau: importance of source and permafrost degradation. *Biogeosciences* **15**, 6637–6648.

Wassenaar L., Aravena R., Fritz P. and Barker J. (1990) Isotopic composition (^{13}C, ^{14}C, ^{2}H) and geochemistry of aquatic humic substances from groundwater. *Org. Geochem.* **15**, 383–396.

Wegner C.-E., Gaspar M., Geesink P., Herrmann M., Marz M. and Küsel K. (2019) Biogeochemical regimes in shallow aquifers reflect the metabolic coupling of the elements nitrogen, sulfur, and carbon. *J. Appl. Environ. Microbiol.* **85**, e02346–02318.

Associate editor: Oleg S. S Pokrovsky